Journal of Alloys and Compounds 680 (2016) 87–94

Contents lists available at ScienceDirect

Journal of Alloys and Compounds

journal homepage: http://www.elsevier.com/locate/jalcom

Peculiarities of magnetic properties of Nd^{3+} ions in the $Nd_{0.5}Gd_{0.5}Fe_3(BO_3)_4$ crystal in the optically excited states $^4(F_{7/2} + S_{3/2})$ and $(^4G_{9/2} + {}^2K_{13/2} + {}^4G_{7/2})$

A.V. Malakhovskii [a, *], S.L. Gnatchenko [b], I.S. Kachur [b], V.G. Piryatinskaya [b], V.L. Temerov [a]

[a] L. V. Kirensky Institute of Physics, Siberian Branch of Russian Academy of Sciences, 660036, Krasnoyarsk, Russian Federation
[b] B. Verkin Institute for Low Temperature Physics and Engineering, National Academy of Sciences of Ukraine, 61103, Kharkov, Ukraine

ARTICLE INFO

Article history:
Received 10 November 2015
Accepted 9 April 2016
Available online 12 April 2016

Keywords:
f-f transitions
Nd^{3+} ion
Excited states
Local magnetic properties

ABSTRACT

Polarized absorption spectra of *f-f* absorption bands $^4I_{9/2} \rightarrow {}^4(F_{7/2} + S_{3/2})$ and $(^4G_{9/2} + {}^2K_{13/2} + {}^4G_{7/2})$ in the Nd^{3+} ion in the $Nd_{0.5}Gd_{0.5}Fe_3(BO_3)_4$ single crystal were studied as a function of temperature in the range of 2–40 K and as a function of magnetic field in the range of 0–65 kOe at 2 K. It was found out that the selection rules for *f-f* electron transitions substantially changed in the magnetically ordered state of the crystal, and they strongly depended on the orientation of the Fe and Nd ions magnetic moments relative to the light polarization. The splitting of the excited states of the Nd^{3+} ion in the exchange field of the Fe sublattice were determined. It was revealed that the value of the exchange splitting (the exchange interaction) did not correlate with the theoretical Landé factor. The Landé factors of the excited states were experimentally found. The local reorientation field induced metamagnetic transitions were observed in the excited states. In some excited states the energetically favorable orientation of the Nd^{3+} ion magnetic moment is opposite to that in the ground state.

1. Introduction

All properties of crystals are totally defined by the electronic structure of ions in the chemical formula of the crystal. The electronically excited ion is similar to the admixture, and, consequently, it changes the local properties of the crystal. A number of phenomena connected with the optical excitation of atoms were observed, e. g., in some rare earth (RE) containing crystals of huntite structure [1–4].

The present work is mainly devoted to study of two phenomena: 1) the influence of the magnetic ordering and magnetic field on the *f-f* electron transitions properties (selection rules, in particular), 2) transformation of the local magnetic and symmetry properties in the excited 4*f* states. Actual problem of the quantum information processing (see e. g., Refs. [5–8]) made the investigations of the local properties of crystals in the optically excited states to be very important. RE containing crystals are widely used in these efforts. So, a change of the local properties near the optically excited atom was used for reading out the information in the quantum memory [6].

Ferroborates of the $RFe_3(BO_3)_4$ type, where R is the RE element, are of the growing interest due to the discovering of the multiferroic properties (i.e. correlation between magnetic, electric and elastic ordering) in many of them [9–13]. The multiferroic effects open the possibility of these materials usage in the new multifunctional devices with the mutual control of magnetic, electric and elastic characteristics. From the viewpoint of the fundamental magnetism, RE ferroborates are of interest due to a wide variety of magnetic properties and phase transitions, which result from the presence of two interacting magnetic subsystems: iron and RE ones [14].

The RE ferroborates has the trigonal huntite-like structure with the space group $R32$ (D_3^7) at high temperatures [15–17]. The unit cell contains three formula units. The RE ions are located at the centers of the trigonal prisms RO_6 (the D_3 symmetry positions). The Fe^{3+} ions are in the C_3 positions inside the octahedrons of oxygen ions. These octahedrons form helicoidal chains along the C_3 axis. With the lowering temperature, some ferroborates undergo a structural phase transition to the $P3_121$ (D_3^4) symmetry phase [17]. It results in the reducing of the RE ion position symmetry to the C_2 one and in appearance of two nonequivalent positions of Fe^{3+} ions

* Corresponding author.
E-mail address: malakha@iph.krasn.ru (A.V. Malakhovskii).

http://dx.doi.org/10.1016/j.jallcom.2016.04.088
0925-8388/

(C_2 and C_1).

All RE ferroborates possess antiferromagnetic (AFM) ordering with the Neel temperature in the range of 30–40 K. The AFM ordering is conditioned by the exchange interaction within the iron subsystem [14]. The magnetic ordering of the RE subsystem is induced by the *f-d* exchange interaction with the Fe subsystem. The RE ions, in turn, due to their magnetic anisotropy, usually determine the direction of the Fe^{3+} magnetic moments in the magnetically ordered state. The RE ferroborates can be easy-axis or easy-plane antiferromagnets. In some of them the reorientation phase transitions occur with the temperature change [18,19].

The $Nd_{0.5}Gd_{0.5}Fe_3(BO_3)_4$ crystal, similar to the pure Nd and Gd ferroborates, is multiferroic [20]. Magnetic properties of the crystal $Nd_{0.5}Gd_{0.5}Fe_3(BO_3)_4$ were investigated in Ref. [21]. Below the $T_N = 32$ K the crystal has an easy-plane AFM structure and the spin-reorientation does not occur down to 2 K. At room temperature, the crystal has *R*32 symmetry and the lattice constants: $a = 9.557$ (7) Å and $c = 7.62$ (1) Å [21]. Any structural phase transitions were not found down to 2 K [21]. In the external magnetic field applied in the basal plane of the crystal a hysteresis in magnetization was found at 1–3.5 kOe. The hysteresis was observed at temperatures $T < 11$ K. Additionally the temperature dependence of the magnetic susceptibility had a singularity at $T = 11$ K (when $H < 1$ kOe). These features were ascribed to the appearance of the static magnetic domains at $T < 11$ K. Spectroscopic studies in the external magnetic field $H \perp C_3$ at 2 K [22] also revealed some features indicating the presence of the domains. The Judd-Ofelt spectroscopic parameters of the $Nd_{0.5}Gd_{0.5}Fe_3(BO_3)_4$ single crystal were determined in Ref. [23]. Some optical and magneto-optical properties of the crystal were earlier studied in Refs. [22,24].

2. Experimental details

$Nd_{0.5}Gd_{0.5}Fe_3(BO_3)_4$ single crystals were grown from the melt solution on the base of $K_2Mo_3O_{10}$ according to Ref. [25]. The absorption spectra were measured with the light propagating normal to the C_3 axis of the crystal for the light electric vector $\vec{E}$ parallel (the π spectrum) and perpendicular (the σ spectrum) to the C_3 axis and the light propagating along the C_3 axis (the α spectrum). The spectral resolution was approximately equal to 1.5 cm^{-1}. The absorption spectra measured in the σ and α polarizations coincide with each other within the limit of the experimental error. This implies that the absorption mainly occurs through the electric dipole mechanism.

Magnetic field was created by a superconducting solenoid with the Helmholtz type coils. The superconducting solenoid with the sample was placed in the liquid helium and all measurements in the magnetic field were fulfilled at $T = 2$ K. For the temperature measurements of absorption spectra a liquid-helium cooled cryostat was used. It had an internal volume filled by the gaseous helium where the sample was placed.

3. Results and discussion

Absorption spectra of the *f-f* transitions were studied in the temperature range of 2–40 K and in the magnetic field 0–65 kOe at the temperature 2 K. Absorption spectra of the studied *f-f* transitions are given in Fig. 1.

The irreducible representations of states (Table 1) were found from polarizations of the transitions and from the selection rules of Table 2. In crystals there is one more characteristic of states: the crystal quantum number μ. Additionally, in crystals with the axial symmetry, wave functions of states can be described by $|J, \pm M_J\rangle$ states of the free atom in a first approximation. In a trigonal crystal, for the states with the half integer total moment there are three

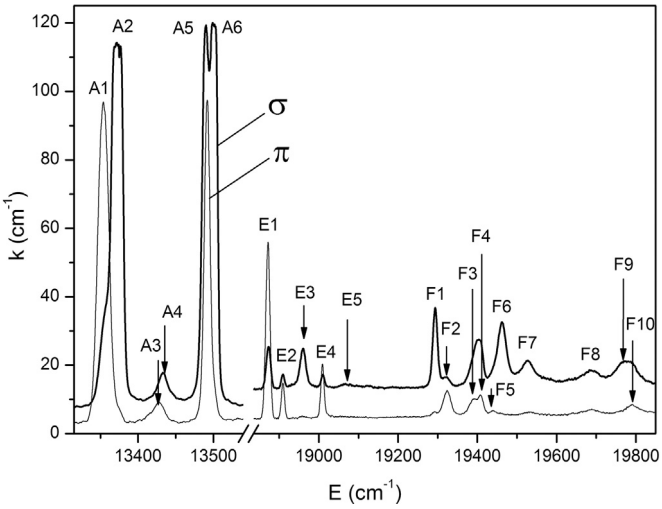

Fig. 1. Polarized absorption spectra of the $^4I_{9/2} \rightarrow {}^4S_{3/2} + {}^4F_{7/2}$ transitions (A band) and of the $^4I_{9/2} \rightarrow {}^4G_{9/2} + {}^4G_{7/2} + {}^2K_{13/2}$ transitions (E + F bands) at $T = 2$ K.

possible values of the crystal quantum number [26]: $\mu = +1/2, -1/2, 3/2$ ($\pm 3/2$), and between values of μ and M_J there is the correspondence:

$$M_J = \pm 1/2, \pm 3/2, \pm 5/2, \pm 7/2, \pm 9/2, \pm 11/2, \pm 13/2$$

$$\mu = \pm 1/2, (\pm 3/2), \mp 1/2, \pm 1/2, (\pm 3/2), \mp 1/2, \pm 1/2 \quad (1)$$

The states with $\mu = \pm 1/2$ correspond to the $E_{1/2}$ states and the states with $\mu = (\pm 3/2)$ correspond to the $E_{3/2}$ states in the D_3 group notations. The values of M_J of the studied states were determined in Ref. [27]. In the $|J, \pm M_J\rangle$ functions approximation, the effective Landé factor of the Kramers doublet along the C_3 axis is [28]:

$$g_{CM} = 2gM_J. \quad (2)$$

Here g is the Landé factor of the free atom. Values of g_{CM} of the studied states are presented in Table 1. In the same Table the theoretical values of g_C in the $NdFe_3(BO_3)_4$ crystal [29] are given. States with the same μ and different M_J (see Eq. (1)) can mix in crystal, and the resulting g_C can be both smaller and larger than g_{CM}.

In the exchange field of the iron sublattice, both the ground and the excited states of the Nd^{3+} ion can be split. So, between components of these splitting four transitions are possible. The main possible diagrams of the splitting and transitions are presented in Fig. 2. In Fig. 2A the splitting between a and b lines, $\Delta E_{12} = (E_a - E_b)$, is equal to the difference between the exchange splitting of the ground and excited states $\Delta E1$ and $\Delta E2$, respectively, while in Fig. 2B it is equal to their sum. In both cases, *a* and *b* transitions are supposed to occur without overturn of the magnetic moment. However, then the favorable moment orientation in the excited state of Fig. 2B diagram will be opposite to that in the ground state. The *c* and *d* transitions in both diagrams occur with the overturn of the magnetic moment, but this does not mean that they are always forbidden (see below).

When $\Delta E2 = 0$, the diagrams of Fig. 2A and B are equivalent and transitions *c* and *d* coincide with the transitions *a* and *b*, respectively, and they have no sense separately (Table 3). This takes place for the states of the $E_{3/2}$ symmetry with $g_\perp = 0$ (Table 1). Then at the lowest temperature the splitting ΔE_{12} will give the exchange splitting of the ground state. However, not all transitions demonstrate the temperature dependent splitting ΔE_{12} connected with the exchange splitting of the ground state. This means that the

Table 1
Parameters of transitions and states. Energies of transitions (E), polarizations and symmetries are given at 40 K. (Details are in the text).

State	Level	E (cm^{-1})	Polar.	Sym.	μ [27]	M_J [27]	g_{CM} [27]	g_C theor. [29]	g_C exper.	$g_\perp$ theor. [29]	$g_\perp$ exper.
$^4F_{7/2}$	A1	13,353	π, σ	$E_{1/2}$	±1/2	±1/2	1.238	0.673	0	3.216	3.62
	A2	13,370	σ	$E_{3/2}$	3/2	±3/2	3.71	3.524		0	
	A3		π, (σ?)	$E_{1/2}$	∓1/2	±5/2	6.19	1.296		4.895	
	A4		(π?)σ	$E_{1/2}$	±1/2	±7/2	8.67	2.141		3.858	
$^4S_{3/2}$	A5	13,488	π, σ	$E_{1/2}$	±1/2	±1/2	2	1.884	0	3.239	
	A6	13,499	σ	$E_{3/2}$	3/2	±3/2	6	5.848		0	
$^4G_{9/2}$	E1	18,872	π, σ	$E_{1/2}$	±1/2	±7/2	1.17	1.784		3.369	
	E2	18,,910	π, σ	$E_{1/2}$	∓1/2	±5/2	5.86	3.026		2.098	
	E3	18,959	≈ σ	$E_{3/2}$	3/2	±3/2	3.515	2.924		0	
	E4	19,010	π, σ	$E_{1/2}$	±1/2	±1/2	8.202	2.081		2.292	
	E5	19,064	σ	$E_{3/2}$	3/2	±9/2	10.54	8.530		0	
$^2K_{13/2}$	F1	19,295	π, σ	$E_{1/2}$	∓1/2	±11/2	10.27	9.760	8.62	0.283	0
$+^4G_{7/2}$	F2	19,323	π, σ	$E_{1/2}$	±1/2	±13/2	12.1	9.860	8.55	0.395	0
	F3	19,389	π, σ	$E_{1/2}$							
	F4	19,408	π, σ	$E_{1/2}$							
	F5	19,438	π, σ	$E_{1/2}$							
	F6	19,461	σ	$E_{3/2}$	3/2	±9/2	8.4	7.030	7.86	0	0
	F7	19,525	π, σ	$E_{1/2}$							
	F8	19,687	π, σ	$E_{1/2}$							
	F9	19,769	σ	$E_{3/2}$	3/2	±3/2(G)	2.952	3.025		0	
	F10	19,793	π, σ	$E_{1/2}$							

Table 2
Selection rules for electric dipole transitions in the D_3 symmetry.

	$E_{1/2}$	$E_{3/2}$
$E_{1/2}$	π, $\sigma(\alpha)$	$\sigma(\alpha)$
$E_{3/2}$	$\sigma(\alpha)$	π

transition from the upper sublevel of the ground state exchange splitting is forbidden. In the studied absorption bands the necessary transitions were not observed, but they were found in the absorption bands $^4I_{9/2} \rightarrow {}^4F_{3/2}$ and $^2H_{9/2}$, and the exchange splitting of the ground state was determined: $\Delta E1 = 9.4$ cm^{-1}. This corresponds to $H_{ex} = 84.4$ kOe, taking into account the theoretical value $g_\perp = 2.385$ for $NdFe_3(BO_3)_4$ [29]. The exchange splitting of the Nd^{3+} ion ground state found in $NdFe_3(BO_3)_4$ was 8.8 cm^{-1} [29].

3.1. $^4I_{9/2} \rightarrow {}^4S_{3/2} + {}^4F_{7/2}$ transitions (A band)

3.1.1. A1 line

The A band spectra were presented in Fig. 1. The geometry of measurements in the magnetic field is presented in Fig. 3. Behavior of the A1aπ and A1cσ lines energies as a function of magnetic field $H \perp C_3$ is depicted in Fig. 4. Magnetic field $H||C_3$ does not change the splitting between these lines, i. e., the C_3 is the hard axis for the excited state A1. According to Table 3, $g_\perp \neq 0$ in the A1 state. Therefore, the splitting of the A1 state in the exchange field of the iron sublattice can exist at $H = 0$. However, it is very small (Fig. 4, Table 3). With the theoretical $g_\perp$ (Table 3) this splitting is equivalent to the effective exchange field $H_E = 3.3$ kOe. Till ~22 kOe (Fig. 4) the orientation of the Nd^{3+} ion magnetic moment in the excited state is defined by the field of anisotropy in the basal plane. The field dependences of the A1a and A1c states energies are crossed (Fig. 4). This means that the energetically favorable orientation of moments in the A1 sublevels at $H = 0$ is opposite to that in the ground state, and Fig. 2B diagram is suitable. The crossing point corresponds to the exchange of the A1a and A1c sublevels positions. The total behavior of the states energies (Fig. 4) is similar to that of metamagnetics [30]. Indeed, if $H_A \geq H_E$, where H_A is the field of anisotropy, then the spin flop transition does not occur. However, when the external magnetic field $H \geq H_A$ the antiferromagnetic phase transforms into the ferromagnetic one in the magnetic field. Thus, we can say that $H_A \approx 22$ kE. The similar phenomenon was observed earlier in Ref. [22] in the $^4I_{9/2} \rightarrow {}^2G_{7/2}$ absorption band of the same crystal (Fig. 4, inset).

The splitting 10.95 cm^{-1} of the A1 line at 65 kOe corresponds to $g_\perp = 3.62$, if the field is counted from the zero. If the field is counted

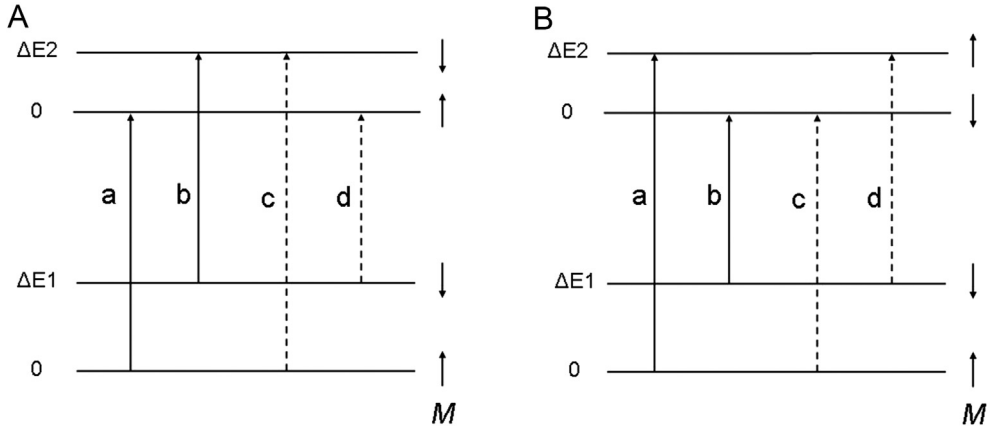

Fig. 2. A and B. Diagrams of transitions in the magnetically ordered state in the zero magnetic field.

Table 3
Polarizations of transitions in the paramagnetic state ($T > T_N$) and of transitions (a, b, c, d) between components of the ground and excite states exchange splitting at $H = 0$, diagrams describing these transitions, the theoretical Landé factor of the Nd^{3+} ion in the basal plane in the $NdFe_3(BO_3)_4$ crystal ($g_\perp$), exchange splitting of the excited states ($\Delta E2$), temperature dependent exchange splitting of absorption lines at 6 K ($\Delta E_{12} = E_a - E_b = \Delta E1 \pm \Delta E2$), the energetically favorable moment orientations in the excited states relative to that in the ground state in the zero magnetic field ($M2$).

Transitions	$T > T_N$	a	b	c	d	Diagram	$g_\perp$ theor. [29]	$\Delta E2$	ΔE_{12}	$M2$
A1 ($\rightarrow E_{1/2}$)	π, σ	π	0	σ	0	2B	3.216	~0.5		(−)
A5 ($\rightarrow E_{1/2}$)	π, σ	π, σ	π, σ?	0	0	2B	3.239	3.0	12.4	(−)
F1 ($\rightarrow E_{1/2}$)	π, σ	π, σ	0	π?, σ	0	2A	0.283	3.7		(+)
F2 ($\rightarrow E_{1/2}$)	π, σ	π, σ	0	π, σ	0	2A	$\neq 0$	~1		
F6 ($\rightarrow E_{3/2}$)	σ	σ	0	–	–	2A, 2B	0	0		
D1 ($\rightarrow E_{1/2}$)	π, σ	π, σ	0	$M \| \sigma$	NCD	2A	0.043	7	–	(−)
D2 ($\rightarrow E_{1/2}$)	π, σ	π	π	σ	?	2B	1.385	2	14	(+)
D3 ($\rightarrow E_{3/2}$)	σ	σ	0	–	–	2A, 2B	0	0	–	
D4 ($\rightarrow E_{1/2}$)	π, σ	π, σ	0	σ	0	2A	2.617	12	–	(+?)
D5 ($\rightarrow E_{1/2}$)	π, σ	π, σ	π	$M \| \pi$	0	2B	0.755	7.5	~17	(+?)
D6 ($\rightarrow E_{1/2}$)	π, σ	π	0	σ	0	2B	1.538	0.4	–	(−)
D7 ($\rightarrow E_{3/2}$)	σ	σ	0	–	–	2A, 2B	0	0	–	

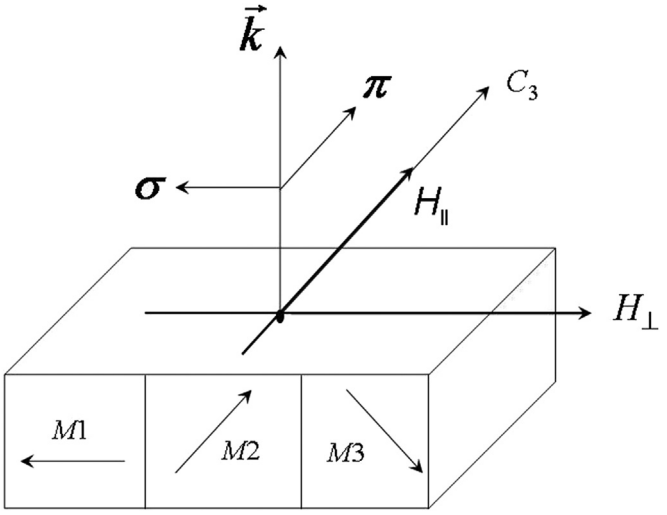

Fig. 3. Geometry of measurements. M1, M2 and M3 are three types of domains in the basal plane.

from the point of the crossing of the lines in Fig. 4, then the splitting corresponds to $g_\perp = 5.46$ (compare with the theoretical value 3.216 for $NdFe_3(BO_3)_4$ in Table 1). Polarizations of the transitions into the A1a and A1c states are different (see Fig. 4) in contrast to what it should be according to symmetry of the A1 state in the D_3 local symmetry of the paramagnetic crystal (Table 3). The A1 line does not split with the decreasing temperature below T_N. This means that transitions from the upper sublevel of the ground state exchange splitting are forbidden (Table 3).

3.1.2. A5 line

The A5π line (Fig. 1) is split with the decreasing temperature below T_N (Fig. 5) due to the exchange splitting of the ground state. This splitting is 12.4 cm^{-1} at 6 K, i. e., it is larger than the exchange splitting of the ground state being equal to 9.4 cm^{-1}. This is possible with the energy diagram of Fig. 2B with the exchange splitting of the excited state of 3.0 cm^{-1}. However the moment orientations in the A5 state sublevels are under the question. Unfortunately, the A5c and A5d lines are not observed. Nevertheless, comparing behavior of the A5a and A1a lines energies in the magnetic field $H \perp C_3$ (Figs. 4 and 6), we infer, that the energetically favorable

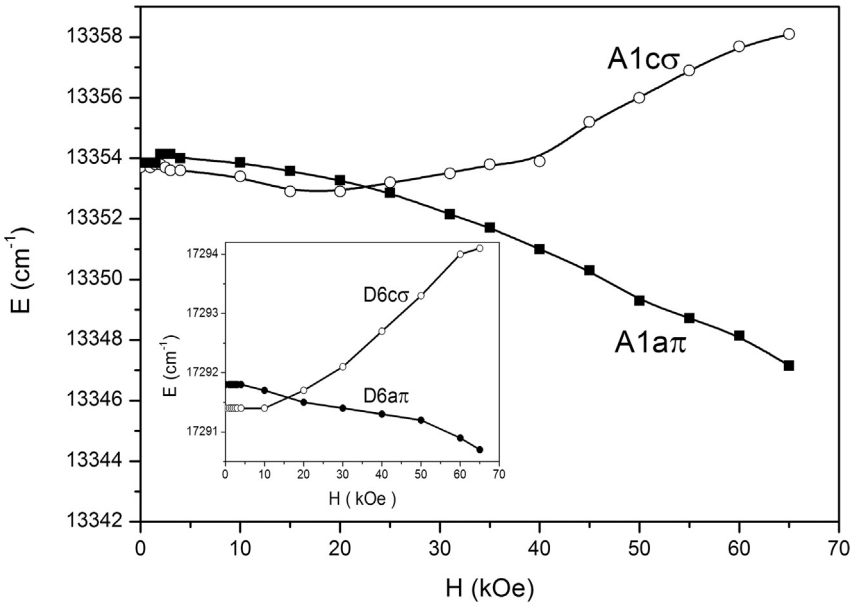

Fig. 4. Energies of the A1 transitions as a function of the magnetic field $H \perp C_3$. Inset: energies of one of the transitions (D6) in the $^4I_{9/2} \rightarrow {}^2G_{7/2}$ absorption band of the same crystal as a function of the magnetic field $H \perp C_3$ [22].

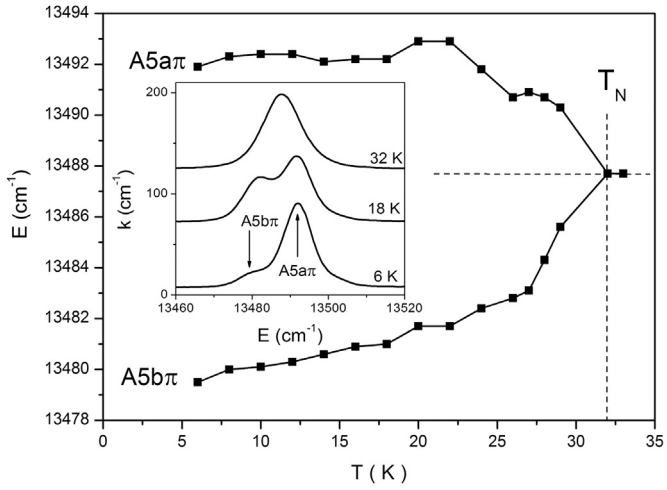

Fig. 5. Temperature dependence of the exchange splitting of the A5π transition. Inset: transformation of the A5π absorption line.

orientation of moments in the A5 sublevels is opposite to that in the ground state, and the diagram of Fig. 2B is totally suitable. At $H = 25$ kOe on the field dependence of the A5a line position a kink is observed (Fig. 6) similar to that observed on the field dependence of the A1 line position (Fig. 4). This can testify to the similar change of the local magnetic state in this excited electron state.

3.1.3. A2 and A6 lines

These lines are too intensive in the σ-polarization to be studied, and they are not active in π-polarization (Fig. 1). They appear in the π-polarization in the magnetic field $H \perp C_3$ (Fig. 6, inset). This means that the changed magnetic structure violates the axial symmetry. The A2 and A6 states have $g_\perp = 0$ (Table 3). Therefore, the splitting of the corresponding absorption lines both in the exchange field and in the external magnetic field $H \perp C_3$ should not exist, but only in the case that the local symmetry in these excited states is the same as in the ground state. However, a kink on the field dependence of the A6π line position (Fig. 6) again testifies to some change of the local magnetic state in this excited electron state.

In the field $H||C_3$ the π-polarized A band spectra practically are not changed that testifies to the strong easy plain anisotropy. The σ-polarized spectra can not be analyzed because of their high intensity.

3.2. $^4I_{9/2} \rightarrow {}^2K_{13/2}+{}^4G_{7/2}+{}^4G_{9/2}$ transitions (E + F band)

The total absorption spectrum of this transition was shown in Fig. 1. Majority of lines of this absorption band do not reveal a dependence on temperature and magnetic field of the both directions. Such situation is possible, if only "a" components of the exchange split transitions are allowed. Only lines F1, F2 and F6 demonstrate a substantial dependence on the magnetic field $H||C_3$. The F1 and F2 states have $E_{1/2}$ symmetry (Table 3) and, consequently, they have $g_\perp \neq 0$ and can have the exchange splitting. In the F1 state it is ~3.7 cm^{-1} (Fig. 7A, Table 3). The F1 and F2 lines reveal no additional splitting in the magnetic field $H \perp C_3$, i. e., this field does not change orientation of the Nd^{3+} ion magnetic moments in the F1 and F2 states because it is hard direction. The F1 energy field dependences in the $H||C_3$ field are not crossed. Therefore Fig. 2A diagram is preferable. Nd^{3+} ion in the F1 state reveals the metamagnetic behavior with H_A~20 kOe. At $H_{||}$>20 kOe the Nd^{3+} magnetic moments in the F1 state change their orientation to the $H||C_3$ direction. The line widths and intensities behavior (Fig. 7B and B inset) confirms the Nd^{3+} magnetic moments reorientation. The splitting 26.1 cm^{-1} at $H = 65$ kOe corresponds to $g_C = 8.62$ that is close to the theoretical values of g_C and g_{CM} (Table 1).

The exchange splitting of the F2π line is not observed. May be, the small difference of the F2σ and F2π lines energies at $H = 0$ (Fig. 8) gives the exchange splitting of the F2 state. The field dependences of the energies and intensities of the F2aπ and F2cπ lines (Fig. 8) show that in the region of 30–50 kOe a reorientation of the Nd^{3+} magnetic moments, to some extent similar to that in the F1 state, takes place. Not linear dependences $E(H)$ can be connected with an inaccuracy of the spectra decomposition into Gauss components. The splitting 25.9 cm^{-1} at $H = 65$ kOe corresponds to $g_C = 8.55$ (Table 1).

The F6 state has $E_{3/2}$ symmetry and the theoretical $g_\perp = 0$

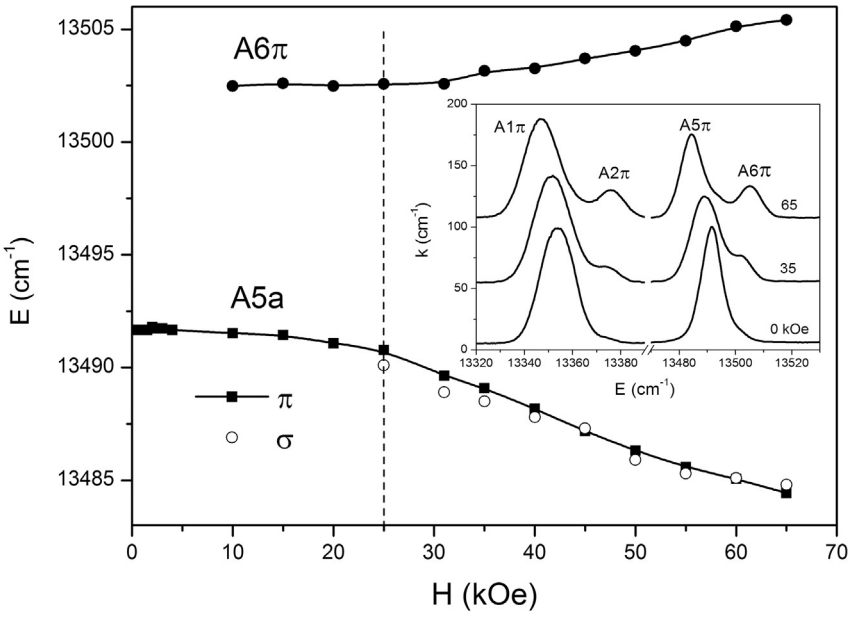

Fig. 6. Energies of the A5 and A6 transitions as a function of the magnetic field $H \perp C_3$. Inset: fragment of the A band spectrum at several magnetic fields $H \perp C_3$.

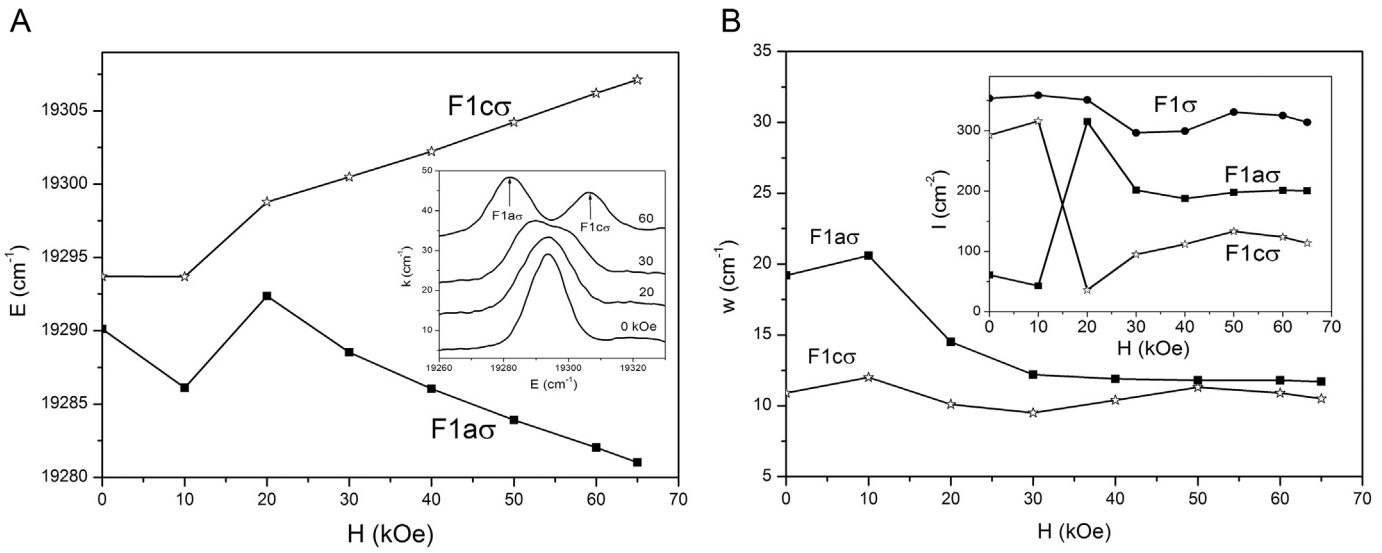

Fig. 7. A. Energies of the F1aσ and F1cσ transitions as a function of the magnetic field $H||C_3$. Inset: transformation of the F1σ spectrum in the magnetic field $H||C_3$. B. Line widths and intensities (inset) of the F1aσ and F1cσ transitions as a function of the magnetic field $H||C_3$.

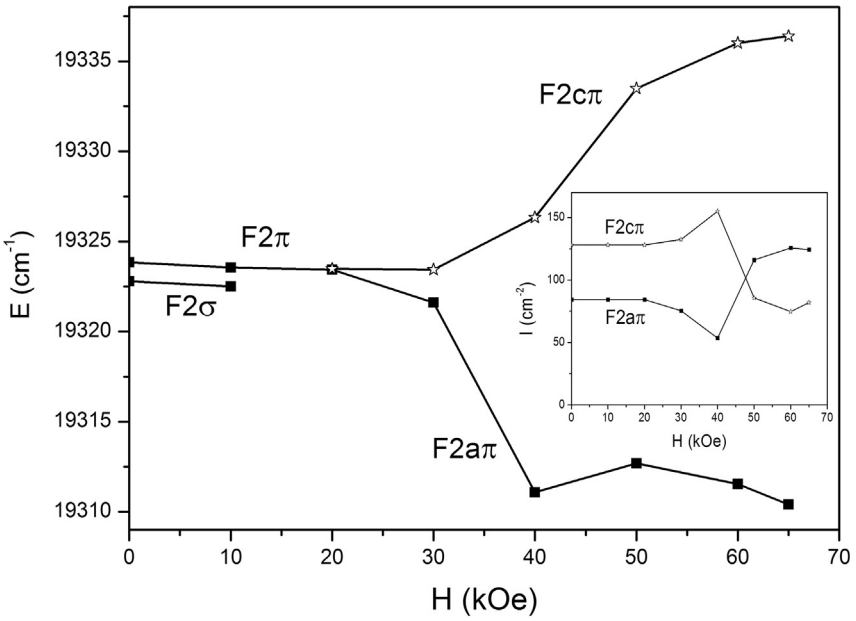

Fig. 8. Energies and intensities (inset) of the F2aπ and F2cπ transitions as a function of the magnetic field $H||C_3$.

(Table 3). Consequently, the exchange splitting of the state should be zero. However, this refers to the ground state local symmetry and can be not valid for the excited state. (Fig. 9). The F6cσ line appears only at $H_{||} = 40$ kOe (Fig. 9). Therefore, it is impossible to retrace the F6cσ transition energy behavior in the lower fields. The kink at 30 kOe in the F6aσ line energy behavior (Fig. 9) and the linear dependence on the magnetic field above 30 kOe apparently testify to the reorientation of magnetic moments to the $H||C_3$ direction similar to that observed in the F1 and F2 states. The splitting 23.8 cm^{-1} at $H = 65$ kOe corresponds to $g = 7.86$ that is close to the theoretical values of g_C and g_{CM} (Table 1).

In conclusion it is necessary to generalize some observed regularities. To give a complete picture we added in Table 3 the results obtained earlier for the transition $^4I_{9/2} \rightarrow {}^4G_{5/2}+{}^2G_{7/2}$ (D-band).

Only polarizations of "a" components of the main part of transitions coincide with those in paramagnetic state of the crystal, but majority of components of all transitions are forbidden at all (Table 3). Some components appear only in magnetic field (Fig. 9) and intensities of transitions substantially depend on the magnetic moment orientation (Fig. 7B inset and Fig. 8 inset). However, at the possible decrease of the local symmetry with the magnetic ordering, all transitions should be allowed at all polarizations. Above observations show, that, first, selection rules by magnetic moment acquire the great importance and, second, the local symmetry is different in different excited states and is unknown.

In Ref. [31] for the $NdFe_3(BO_3)_4$ crystal there were suggested the following Hamiltonians of Nd and Fe ions from the *i*th sublattice (i = 1,2) in the presence of magnetic field:

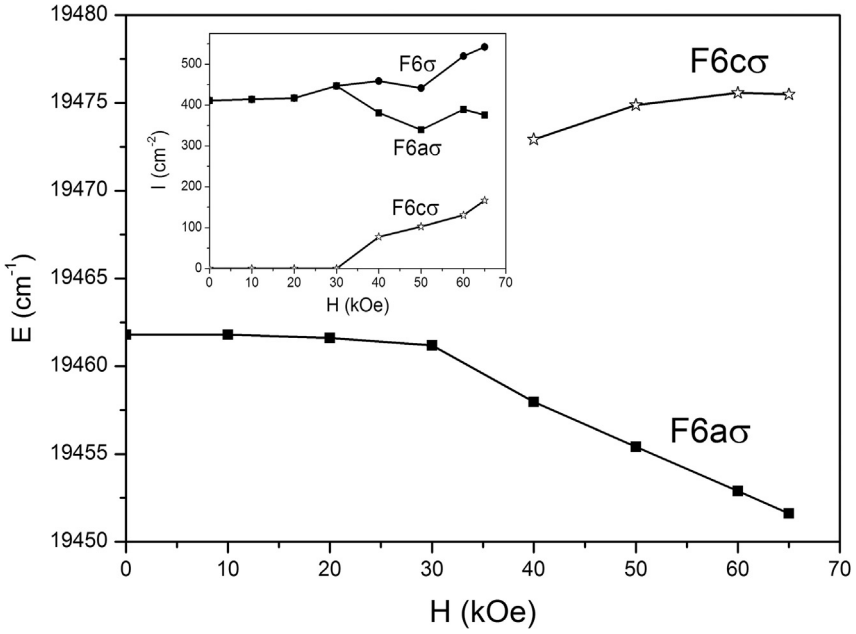

Fig. 9. Energies and intensities (inset) of the F6aσ and F6cσ transitions as a function of the magnetic field $H||C_3$.

$$\widehat{H}_i(Nd) = \widehat{H}^i_{CF} - g_J\mu_B\vec{J}_i\cdot\left(\vec{H} + \lambda_{fd}\vec{M}_i\right), \quad (3)$$

$$\widehat{H}_i(Fe) = -g_S\mu_B\vec{S}_i\cdot\left(\vec{H} + \lambda\vec{M}_j + \lambda_{fd}\vec{m}_i\right). \quad (4)$$

Here $\widehat{H}_{CF}$ is the crystal field Hamiltonian, whose form is determined by the symmetry of the local environment of an Nd ion, g_J is the Landé factor and $\widehat{J}_i$ is the operator of the angular momentum of the Nd ion, $g_S = 2$ is the Landé factor and $\vec{S}_i$ is the operator of the spin moment of an iron atom, $\lambda_{fd} < 0$ and $\lambda < 0$ are the molecular constants of the AFM interactions Nd–Fe and Fe–Fe, respectively, $\vec{M}_i$ and $\vec{m}_i$ are the magnetic moments of the Fe and Nd ions, respectively. Hamiltonians (3) and (4) are written, taking into account that according to Ref. [18] RE ions in ferroborates do not interact with iron ions positioned in the same crystal plane, but reveal the AFM interaction with the iron ions in the adjacent planes. Interactions inside the RE subsystem is not taken into account since it is negligibly small. Parameters of the CF in $NdFe_3(BO_3)_4$ were determined, basing on its absorption spectra [29]. These parameters permitted to find the Landé factors of Nd ion and magnetic properties of the $NdFe_3(BO_3)_4$ crystal [29,31]. Crystal structure of the $Nd_{0.5}Gd_{0.5}Fe_3(BO_3)_4$ crystal is identical to that of the $NdFe_3(BO_3)_4$, and absorption spectra of these crystals are very close. Therefore we used the Landé factors obtained as a first approximation (Tables 1 and 3). In some cases they are close to the experimentally found ones, but, they are substantially different for g_C in the A1 and A5 states and for $g_\perp$ in the F1 and F2 states (Table 1). Consequently, the local magnetic anisotropy of the Nd^{3+} ion in these states substantially differs from the predicted ones. This testifies to the deviation of the local CF in the excited states of the Nd ion from that in the ground state. Possibility of the photo-induced single-ion magnetic anisotropy was theoretically considered, e. g., in Ref. [32]. The exchange interactions in (3) and (4) remain to be the parameters found experimentally.

The exchange field of the Fe sublattice is directed perpendicular to the C_3 axis. Therefore, the exchange splitting of the excited Nd^{3+} states with $g_\perp = 0$ should be zero. It is really so (see Table 3). However, the value of the exchange splitting (the exchange interaction) does not correlate with the theoretical Landé factor $g_\perp$ of the Nd^{3+} ion (Table 3). It is necessary to note that the Hamiltonian (3) does not take into account the anisotropic and anti symmetric exchange, which can be one of the reasons of the peculiar magnetic properties of the Nd ion in the excited states. In particular, the anti symmetric exchange provides the mutually perpendicular orientation of the magnetic moments of the Fe and Nd ions.

In general, the local magnetic properties in the vicinity of the excited ion substantially depend on its electron state. From the above consideration it is clear that this is connected with the change of the local interaction of the excited ion with the environment. Thus, the knowledge of the crystal field in the ground state can not provide the theoretical prediction of the local magnetic and other properties in the excited states.

4. Summary

Polarized absorption spectra of the *f-f* absorption bands $^4I_{9/2} \rightarrow {}^4(F_{7/2} + S_{3/2})$ and $({}^4G_{9/2} + {}^2K_{13/2} + {}^4G_{7/2})$ in the Nd^{3+} ion in the $Nd_{0.5}Gd_{0.5}Fe_3(BO_3)_4$ single crystal were studied as a function of temperature in the range of 2–40 K and as a function of magnetic field in the range of 0–65 kOe at 2 K. In the magnetically ordered state of the crystal, the splitting of the excited states of the Nd^{3+} ion in the exchange field of the Fe sublattice were determined. The value of the exchange splitting (the exchange interaction) does not correlate with the theoretical Landé factor $g_\perp$ of the Nd^{3+} ion. The Landé factors of the excited states were experimentally found. In some states they substantially differ from the theoretically predicted ones. This testifies to the deviation of the local CF and magnetic anisotropy in the excited states of the Nd ion from that in the ground state. The local reorientation field induced metamagnetic transitions were observed. In some excited states the energetically favorable orientation of the Nd^{3+} ion magnetic moment is opposite to that in the ground state.

It was found out that the selection rules for the electron transitions substantially changed as compared with the paramagnetic state of the crystal. They are different for the different transitions with the same symmetry in the paramagnetic state of the crystal (Table 3), and they strongly depend on the orientation of the Fe and

Nd ions magnetic moments relative to the light polarization. Some transitions appear only in the magnetic field. It is also worth noting that majority of the studied excited states has identical symmetry $E_{1/2}$ in the paramagnetic state of the crystal, but they have a great variety of the local magnetic properties. There can be two sources of these features. First, these states refer to different multiplets and (or) have different M_J in the $|J, \pm M_J\rangle$ representation (Table 1). Second, in spite of the axial crystal symmetry, the magnetic moments in the ground state are in the plane perpendicular to the C_3 axis. Therefore, they create one more quantization axis besides the C_3 one, and, consequently, they create the peculiar selection rules for the electron transitions, which depend also on the excited states because the electronically excited atom modifies the local symmetry and magnetic properties of the crystal.

Acknowledgements

The work was supported by the Russian Foundation for Basic Researches grant 16-02-00273 and by the President of Russia grant No Nsh-2886.2014.2.

References

[1] A.V. Malakhovskii, A.L. Sukhachev, S.L. Gnatchenko, I.S. Kachur, V.G. Piryatinskaya, V.L. Temerov, A.S. Krylov, I.S. Edelman, J. Alloys Comp. 476 (2009) 64.
[2] A.V. Malakhovskii, S.L. Gnatchenko, I.S. Kachur, V.G. Piryatinskaya, A.L. Sukhachev, V.L. Temerov, Eur. Phys. J. B 80 (2011) 1.
[3] A.V. Malakhovskii, S.L. Gnatchenko, I.S. Kachur, V.G. Piryatinskaya, A.L. Sukhachev, I.A. Gudim, J. Alloys Compd. 542 (2012) 157.
[4] A.V. Malakhovskii, S.L. Gnatchenko, I.S. Kachur, V.G. Piryatinskaya, A.L. Sukhachev, A.E. Sokolov, A. Ya. Strokova, A.V. Kartashev, V.L. Temerov, Crystallogr. Rep. 58 (2013) 135.
[5] J.J. Longdell, M.J. Sellars, Phys. Rev. A 69 (2004) 032307.
[6] J.H. Wesenberg, K. Mølmer, L. Rippe, S. Kröll, Phys. Rev. A 75 (2007) 012304.
[7] A.V. Kimel, A. Kirilyuk, T. Rasing, Laser Phot. Rev. 1 (2007) 275.
[8] A.I. Lvovsky, B.C. Sanders, W. Tittel, Nat. Photonics 3 (2009) 706.
[9] A.K. Zvezdin, S.S. Krotov, A.M. Kadomtseva, G.P. Vorob'ev, Yu.F. Popov, A.P. Pyatakov, L.N. Bezmaternykh, E.A. Popova, Pis'ma v ZhETF 81 (2005) 335 [JETP Lett. 81 (2005) 272].
[10] A.K. Zvezdin, G.P. Vorob'ev, A.M. Kadomtseva, Yu.F. Popov, A.P. Pyatakov, L.N. Bezmaternykh, A.V. Kuvardin, E.A. Popova, Pis'ma v ZhETF 83 (2006) 600 [JETP Lett. 83 (2006) 509].
[11] F. Yen, B. Lorenz, Y.Y. Sun, C.W. Chu, L.N. Bezmaternykh, A.N. Vasiliev, Phys. Rev. B 73 (2006) 054435.
[12] R.P. Chaudhury, F. Yen, B. Lorenz, Y.Y. Sun, L.N. Bezmaternykh, V.L. Temerov, C.W. Chu, Phys. Rev. B 80 (2009) 104424.
[13] A.M. Kadomtseva, Yu.F. Popov, G.P. Vorob'ev, A.P. Pyatakov, S.S. Krotov, P.I. Kamilov, V.Yu. Ivanov, A.A. Mukhin, A.K. Zvezdin, L.N. Bezmaternykh, I.A. Gudim, V.L. Temerov, Fiz. Nizk. Temp. 36 (2010) 640 [Low Temp. Phys. 36 (2010) 511].
[14] A.N. Vasiliev, E.A. Popova, Fiz. Nizk. Temp. 32 (2006) 968 [Low Temp. Phys. 32 (2006) 735].
[15] J.C. Joubert, W. White, R. Roy, J. Appl. Cryst. 1 (1968) 318.
[16] J.A. Campá, C. Cascales, E. Gutiérrez-Puebla, M.A. Monge, I. Rasines, C. Ruíz-Valero, Chem. Mater. 9 (1997) 237.
[17] S.A. Klimin, D. Fausti, A. Meetsma, L.N. Bezmaternykh, P.H.M. van Loosdrecht, T.T.M. Palstra, Acta Crystallogr. B 61 (2005) 481.
[18] A.I. Pankrats, G.A. Petrakovsky, L.N. Bezmaternykh, O.A. Bayukov, ZhETF 126 (2004) 887 [JETP 99 (2004) 766].
[19] C. Ritter, A. Vorotynov, A. Pankrats, G. Petrakovskii, V. Temerov, I. Gudim, R. Szymczak, J. Phys. Condens. Matter 20 (2008) 365209.
[20] A.M. Kadomtseva, Yu. F. Popov, G.P. Vorob'ev, A.A. Mukhin, V. Yu. Ivanov, A.M. Kuz'menko, A.S. Prokhorov, L.N. Bezmaternykh, V.L. Temerov, I.A. Gudim, in: Proceedings of the XXI International Conference "New in Magnetism and Magnetic Materials," Moscow, 2009, p. 316.
[21] A.V. Malakhovskii, E.V. Eremin, D.A. Velikanov, A.V. Kartashev, A.D. Vasil'ev, I.A. Gudim, Fiz. Tverd. Tela 53 (2011) 1929 [Phys. Solid State 53 (2011) 2032].
[22] A.V. Malakhovskii, S.L. Gnatchenko, I.S. Kachur, V.G. Piryatinskaya, A.L. Sukhachev, V.L. Temerov, JMMM 375 (2015) 153.
[23] A.V. Malakhovskii, A.L. Sukhachev, A.A. Leont'ev, I.A. Gudim, A.S. Krylov, A.S. Aleksandrovsky, J. Alloys Compd. 529 (2012) 38.
[24] A.V. Malakhovskii, S.L. Gnatchenko, I.S. Kachur, V.G. Piryatinskaya, A.L. Sukhachev, I.A. Gudim, J. Alloys Compd. 542 (2012) 157.
[25] A.D. Balaev, L.N. Bezmaternykh, I.A. Gudim, V.L. Temerov, S.G. Ovchinnikov, S.A. Kharlamova, J. Magn. Magn. Mater. 258–259 (2003) 532.
[26] M.A. El'yashevitch, Spectra of Rear Earths, Moskow, 1953 (in Russian).
[27] A.V. Malakhovskii, S.L. Gnatchenko, I.S. Kachur, V.G. Piryatinskaya, A.L. Sukhachev, V.L. Temerov, J. Magn. Magn. Mater. (2015). http://dx.doi.org/10.1016/j.
[28] A.V. Malakhovskii, A.L. Sukhachev, A. Yu. Strokova, I.A. Gudim, Phys. Rev. B 88 (2013) 075103.
[29] M.N. Popova, E.P. Chukalina, T.N. Stanislavchuk, B.Z. Malkin, A.R. Zakirov, E. Antic-Fidancev, E.A. Popova, L.N. Bezmaternykh, V.L. Temerov, Phys. Rev. B 75 (2007) 224435.
[30] E. Stryjevski, N. Giordano, Adv. Phys. 26 (1977) 487.
[31] D.V. Volkov, E.A. Popova, N.P. Kolmakova, A.A. Demidov, N. Tristan, Yu. Skourski, B. Buechner, I.A. Gudim, L.N. Bezmaternykh, JMMM 316 (2007) e717.
[32] V.V. Eremenko, N.E. Kaner, Yu. G. Litvinenko, V.V. Shapiro, Sov. Phys. JETP 57 (1983) 1312.